

International Conference on Space Optics—ICSO 2018

Chania, Greece

9–12 October 2018

Edited by Zoran Sodnik, Nikos Karafolas, and Bruno Cugny



Analysis and control of light scattered by optical components for space applications

M. Zerrad

M. Lequime

C. Amra



International Conference on Space Optics — ICSO 2018, edited by Zoran Sodnik, Nikos Karafolas, Bruno Cugny, Proc. of SPIE Vol. 11180, 1118086 · © 2018 ESA and CNES · CCC code: 0277-786X/18/\$18 · doi: 10.1117/12.2536213

Analysis and control of light scattered by optical components for space applications

M. Zerrad*, M. Lequime, C. Amra
Aix Marseille Univ, CNRS, Centrale Marseille, Institut Fresnel, Marseille, France

ABSTRACT

Space applications require more and more demanding optical functions. This evolution led to the development of new generation of optical components with extreme performances in terms of scattering level, roughness, localized defects, spectral evolution of performances, coherent backscattering.... In this context, optical components produced for space applications present an increasing complexity with extreme specifications. As a consequence, new problematics specific to this generation of components appeared and among these, the management of light scattered by these components remains a significant challenge.

For example, for complex optical coatings (typically with more than 100 interfaces), the scattering response of the component is not directly correlated to the substrate spectrum, as it is the case for simple coatings (less than 40 layers). For this reason, an accurate modelling of light scattered by complex optical coatings requires a global analysis taking into account different parameters from the design and manufacturing to the conditions of use of the component.

We will present in this paper the last developments performed by the Scattering Group of Institut Fresnel for the modelling and the metrology of light scattered by complex optical components for space applications.

A specific care will be given to recent studies performed on narrow band filters for earth observation and high performances mirrors. For each of these applications, the specific problematics and corresponding challenges will be presented and experimental and numerical results will be detailed. The agreement between metrology and modelling will be highlighted.

Keywords: Optical coatings, Light scattering, Metrology, Modeling, Straylight

1. INTRODUCTION

New generations of optical coatings present an increasing complexity in order to face more and more drastic applications. As a consequence, their specifications become extreme and require to develop improved optimal metrology. On the other hand, new questions are raised and concern the scattering losses of these complex coatings. Actually, the corresponding scattering patterns exhibit spectral and angular lobes which alter the coating performances in the final application. We present in this paper the last development performed by the Institut Fresnel on the modelization of the spectral and angular scattering patterns of complex optical coatings. We show that if we take into account the substrate role and the coating formula, predicted BSDF are in good agreement with scattering patterns measured with the help of a new Spectral and Angular Light Scattering characterization Apparatus (*SALSA*) developed by the laboratory [1-3].

2. MODELING OF ELECTROMAGNETIC OPTICAL FIELD SCATTERED BY INTERFERENTIAL COATINGS

Previous works [4-14] have allowed to develop theoretical models to predict scattering losses of optical components. Scalar theories [15] give a first approximation of the total scattered light S for low roughnesses. Relationship between total scattering (S), the reflection factor (R) and the root mean square (rms) roughness δ of the surface is given by equation (1) for an illumination at wavelength λ and angle i_0 in an ambient medium of index n_0 .

$$S / R = \left(4\pi n_0 \frac{\delta}{\lambda} \cos i_0 \right)^2 \quad (1)$$

[*myriam.zerrad@fresnel.fr](mailto:myriam.zerrad@fresnel.fr) ; www.fresnel.fr/concept

This formula is valid in the case of single surfaces and can be generalized to simple correlated coatings, but suffers from limitations which have been overcome with the development of electromagnetic theories [4, 6, 16, 17]. Some key points to consider are to take into account the polarization and to access to the angular repartition of the scattered intensity. Because of their low roughness-to-wavelength ratio, for high precision optical components the scattered field can be assumed to equal its first order approximation and expressed as a function of the spatial pulsation $\vec{\sigma}$. As a consequence, the Angular Resolved Scattering pattern (ARS) can be formulated following equation (2) :

$$ARS(\vec{\sigma}) = D_s(\vec{\sigma}) \gamma_s(\vec{\sigma}) \quad (2)$$

where D_s is an electromagnetic term [4] that takes into account the illumination conditions (λ , i_0 , polarization), and γ_s is the power spectral density of the surface topography $h(x,y)$ defined by equation (3):

$$\gamma_s(\vec{\sigma}) = \frac{1}{\Sigma} |\tilde{h}(x,y)|^2 \quad (3)$$

where symbol \sim is for the spatial Fourier Transform and Σ is the area of illuminated surface.

The spatial pulsation $\vec{\sigma}$ of modulus $\sigma = \frac{2\pi n_0}{\lambda} \sin \theta$ is defined as illustrated Figure 1 as a function of the normal and azimuthal scattering angles θ and ϕ .

The first order model was extended to the management of multilayer planar structures. In this case, the scattered intensity is written as :

$$ARS(\vec{\sigma}) = \sum_{p,q} C_p(\vec{\sigma}) C_q^*(\vec{\sigma}) \gamma_{pq}(\vec{\sigma}) \quad (4)$$

where p and q are subscript indices for the N interfaces, $*$ is for the complex conjugate value and γ_{pq} is the Fourier transform of the cross-correlation function between profiles of interfaces p and q as defined by equation (5).

$$\gamma_{pq} = \frac{1}{\Sigma} TF[h_p(x,y) \otimes h_q(-x,-y)] \quad (5)$$

with \otimes the convolution product.

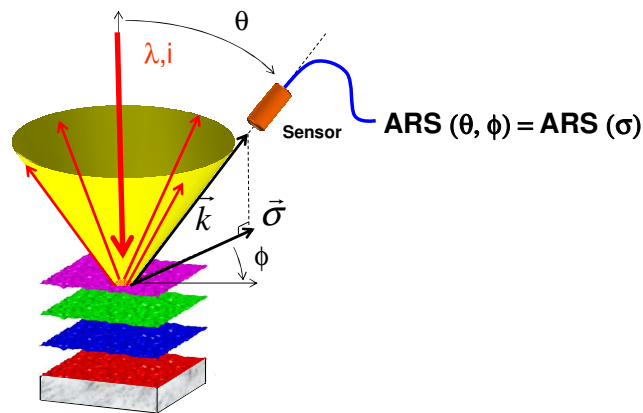


Figure 1: Definition of scattering angles (θ , ϕ) and spatial pulsation $\vec{\sigma}$

At this step, it is usual to introduce a normalized cross-correlation coefficient α_{pq} between interfaces p and q as follows:

$$\gamma_{pq} = \alpha_{pq} \gamma_q \quad (6)$$

The resulting general expression of scattered intensity is then given equation (7).

$$ARS(\vec{\sigma}) = \sum_{p,q} C_{pq}(\vec{\sigma}) \alpha_{pq}(\vec{\sigma}) \gamma_q(\vec{\sigma}) \quad (7)$$

A similar theory has been developed in the case of bulk scattering [4, 18] but will not be considered here because, for high quality optical coatings, surface roughness can be considered as the main source of scattering losses.

The expression (7) highlights the effects of the different physical parameters one has to take into account for an accurate prediction of scattering losses. We have seen in previous papers [13, 14] that every part of the synthesis and production line is important and has to be considered independently. First, γ_s , the PSD of the substrate can be directly characterized by a suited multiscale analysis before deposition. Then, the qualification of the deposition technology is required to define the optical indices and the correlation coefficients α_{pq} . The knowledge of these coefficients added to the analysis of the substrate will allow us to access the different spectra γ_q . The coating formula is, of course, a key parameter in the scattering behavior. It will act on the value of C_{pq} coefficients.

3. SUBSTRATE ANALYSIS

The first element of any optical device is the substrate and its choice is a key point to guarantee the performances of the coating. To analyze the role of the substrate, we first have to define the concept of spatial bandpass. As seen in part 1, all parameters which manage the scattering patterns are function of the spatial frequency $\vec{\sigma}$. In case of in-plane analysis ($\phi = 0$) the vector $\vec{\sigma}$ can be replaced by its modulus σ . For optical waves, at wavelength λ and angle θ , this modulus is defined as:

$$\sigma = \frac{2\pi n_0}{\lambda} \sin \theta \quad (8)$$

To quantify the effect of the substrate topography, we need to realize a mapping of the topography with quantitative microscopy and then to extract the corresponding PSD. An example of microscopic multiscale analysis is given Figure 2 for a fused silica substrate with a P4 polishing quality. The study is said to be multiscale because the topography is measured on a panel of band-passes, that is, with different spatial resolutions. The White Light Interferometer Zygo New View 7300 available at the Institut Fresnel is perfectly suited for that kind of study because it allows to scan a large panel of windows size and resolutions and, as a consequence, a large range of spatial frequencies.

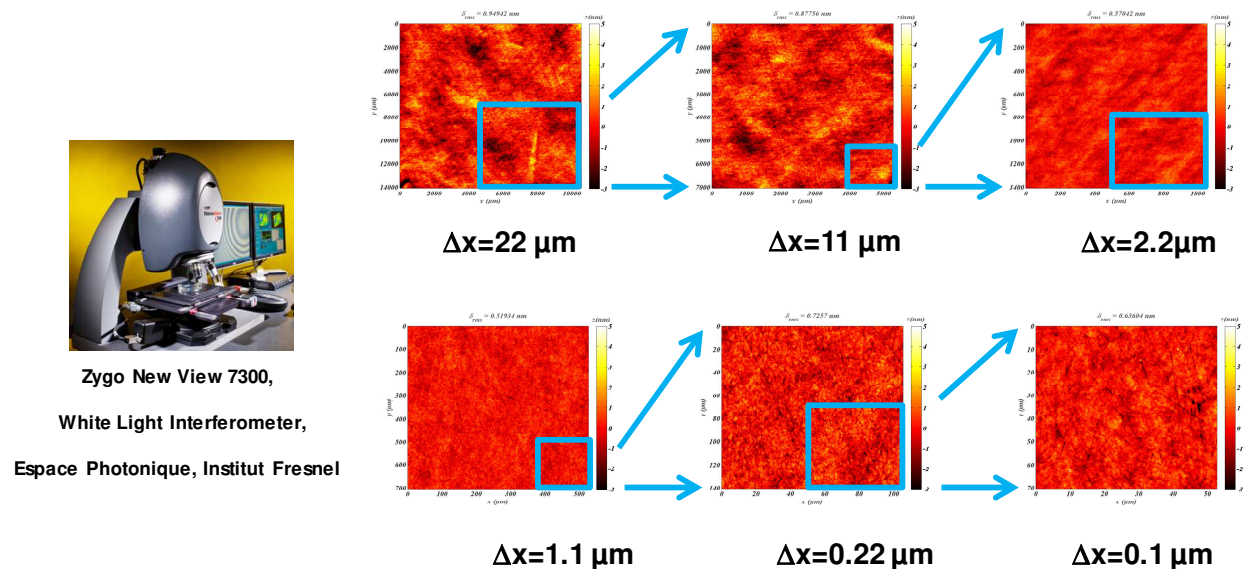


Figure 2: Multiscale characterization of a fused silica substrate with a P4 polishing quality performed Zygo New View 7300 White Light Interferometer based in the Espace Photonique platform of the Institut Fresnel

More precisely, for a mapping measured on a surface $L \times L$ with a resolution Δx , the Shannon Nyquist criterion imposes that the minimal and maximal corresponding spatial pulsations are respectively:

$$\begin{cases} \sigma_{M,\min} = \frac{2\pi}{L} \\ \sigma_{M,\max} = \frac{2\pi}{\Delta x} \end{cases} \quad (9)$$

where index M is for Microscopy.

We can now calculate the PSD of the substrate from formula (3) and plot them on the corresponding band-passes as illustrated Figure 3. As expected [19] the roughness spectra follow a fractal behavior and overlap on the different band-passes.

At this step we need to remind that the global aim of this study is to calculate scattering losses of the global component, so we have to define the bandpass of interest for the scattering analysis and to consider the PSD on this bandpass. To be quantitative, a BSDF (Bidirectionnal Scattering Distribution Function) measured on the Silicon detection spectral range ($\lambda=400$ nm to 1000 nm) on the whole reflected half space ($\theta=1^\circ$ to 90°) covers a bandpass BP_S defined as follow:

$$BP_S = [\sigma_{S,\min}; \sigma_{S,\max}] \quad (10)$$

where index S is for Scattering abbreviation and:

$$\begin{cases} \sigma_{S,\min} = \frac{2\pi n_0}{\lambda} \sin \theta_{\min} \\ \sigma_{S,\max} = \frac{2\pi n_0}{\lambda} \sin \theta_{\max} \end{cases} \quad (11)$$

The limits of BP_S are plotted on Figure 3 for 2 different wavelengths.

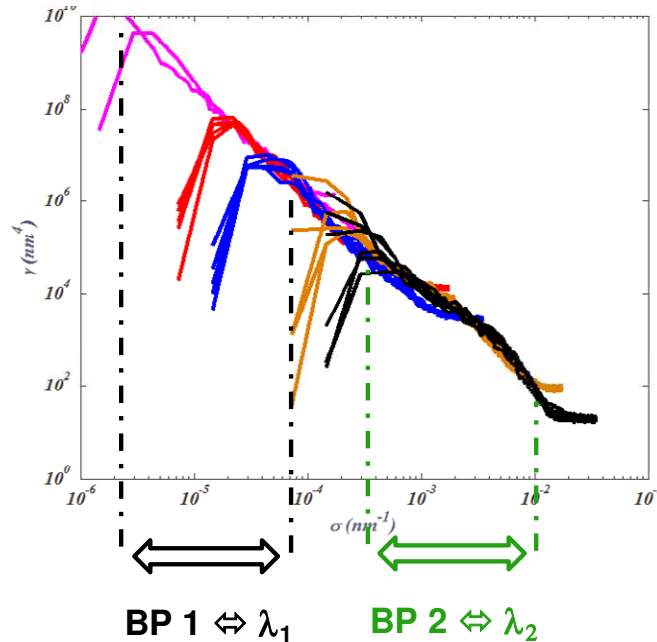


Figure 3: Power Spectral Density function γ calculated from measurements given Figure 2.

From this DSP, we can calculate the spectral and angular repartition of the intensity of the light scattered by the substrate using formula (2). The corresponding mappings are plotted Figure 4 for s (left) and p (right) polarization. We can see Figure 6 the BRDF pattern extracted at 633 nm where θ is the scattering angle as it is defined Figure 5.

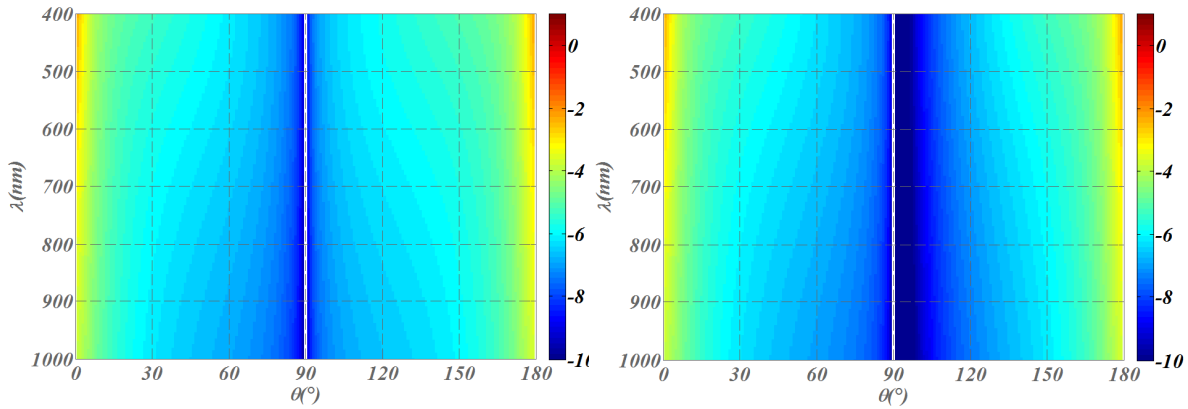


Figure 4: Modelization of the spectral and angular pattern of the intensity of light scattered by substrate measured Figure 2 under S polarization (left) and P polarization (right). Color scale is for the log of the scattered intensity.

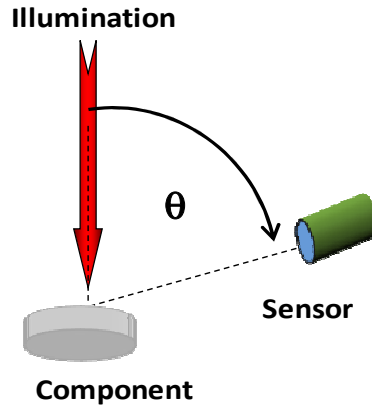


Figure 5: Configuration for the measurement of a BRDF pattern

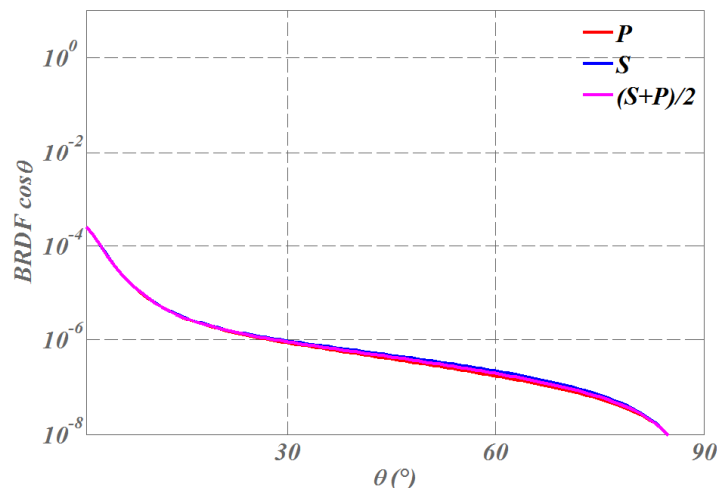


Figure 6: Modelization of the angular pattern of the intensity of light scattered in the reflected half space by the substrate measured Figure 2 under S and P polarization. Calculation is made for $\lambda=633$ nm

4. STRAYLIGHT & MIRRORS

Reflective coatings or mirrors are classical optical functions and their scattering response is now well mastered. If we consider a mirror with 17 dielectric layers. It is an alternance of high and low refractive index material, respectively TiO₂ and SiO₂. All thicknesses are quarter-wave for an illumination wavelength of 633 nm under normal incidence and the corresponding transmission and reflexion functions are plotted Figure 7.

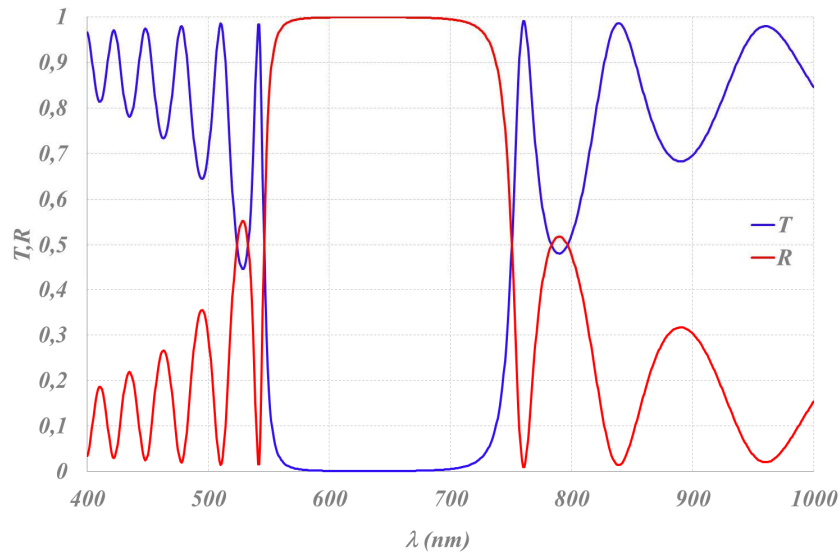


Figure 7 : Transmission and reflexion coefficient of a M17 mirror quarterwave at the wavelength of 633 nm

Let us now consider that we deposit this mirror on the substrate characterized in section 3. To consider both the coating formula and the substrate, we can use the formula (7) to calculate the angular and spectral variations of the scattered intensity. The resulting scattered intensity is plotted Figure 8

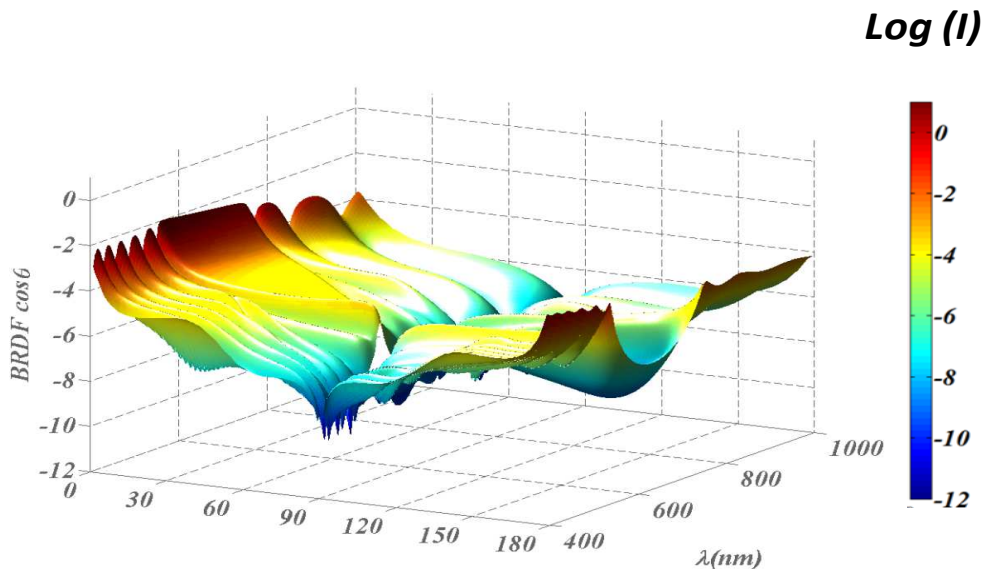


Figure 8: Modelization of the spectral and angular pattern of the intensity of light scattered by a 17 layers mirror assumed to be deposited on the substrate measured Figure 2 under S polarization (left) and P polarization (right). Color scale is for the log of the scattered intensity and vertical scale is logarithmic.

We can extract from these data, the BRDF for the central wavelength of the mirror, 633 nm which is given Figure 9. This curve has to be compared to the scattering pattern obtained for the uncoated substrate and plotted Figure 6. We can

notice at this step that the scattering level is much higher for the mirror whereas the angular behaviour of scattered light is quite similar than for the uncoated substrate.

We this example, we have an illustration of the fact that, for simple coating formulas, the angular behaviour of scattered intensity is imposed by the topography of the interfaces, whereas, the spectral evolution is managed by the transmission and reflexion functions.

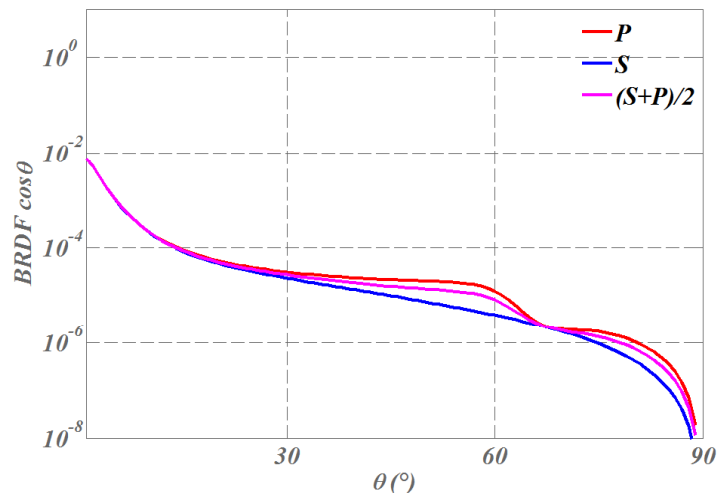


Figure 9: Modelization of the angular pattern of the intensity of light scattered in the reflected half space by a 17 layers mirror assumed to be deposited on the substrate measured Figure 2 under S and P polarization. Calculation is made for $\lambda=633$ nm

To illustrate the relevancy of the models, we propose Figure 10 a comparative plot, in the case of a multielectric mirror, of the BRDF calculated (blue line) and measured (red dots) with the SALSA instrument [1, 2, 13, 14, 20]. (SALSA is for Spectral and Angular Light Scattering characterization Apparatus). Calculation and measurement have been done at the wavelength of 900 nm for an unpolarized illumination. We can notice here that the agreement between modelling and metrology is excellent without any fit on the calculation parameters .

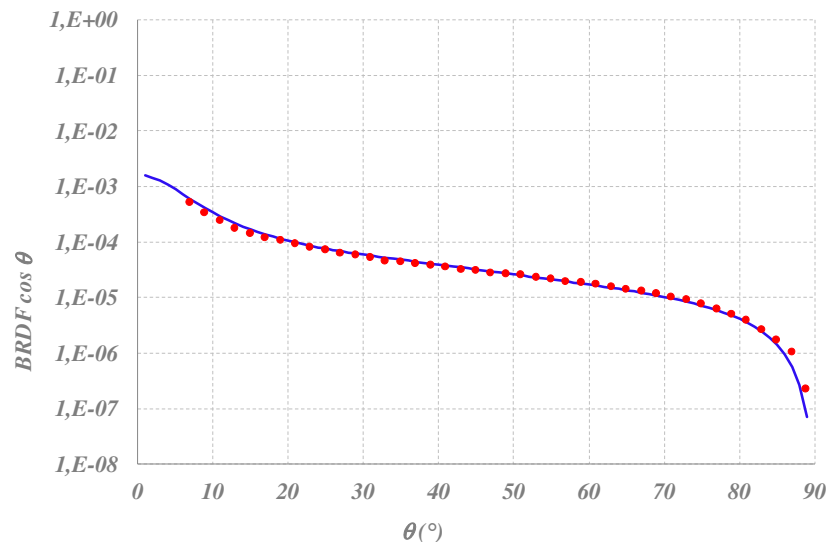


Figure 10 : Modelization (blue line) and measurement (red dots) of the BRDF pattern of a mirror under unpolarized illumination at 900 nm.

5. COMPLEX FILTERS AND LARGE ANGLE SCATTERING

We will now consider the specific case of complex optical coatings. They can be necessary for highly demanding optical functions and to illustrate this problematic, we will consider narrow band filters. Three examples of narrow band filters are given Figure 11. They are all centred at 633 nm and present increasing level of performances and, as a consequence, an increasing complexity. Filter (a) is a Fabry-Perot cavity (~40 layers), Filter (b) is a multi-cavities Fabry-Perot filter (~60 layers) and (c) is the same as (b) with self-blocking filters to enlarge the rejection spectral width (> 100 layers). For each of them, the transmission of the filter is plotted as a function of the wavelength on the left and the spectral and angular evolution of the scattered intensity is given on the right.

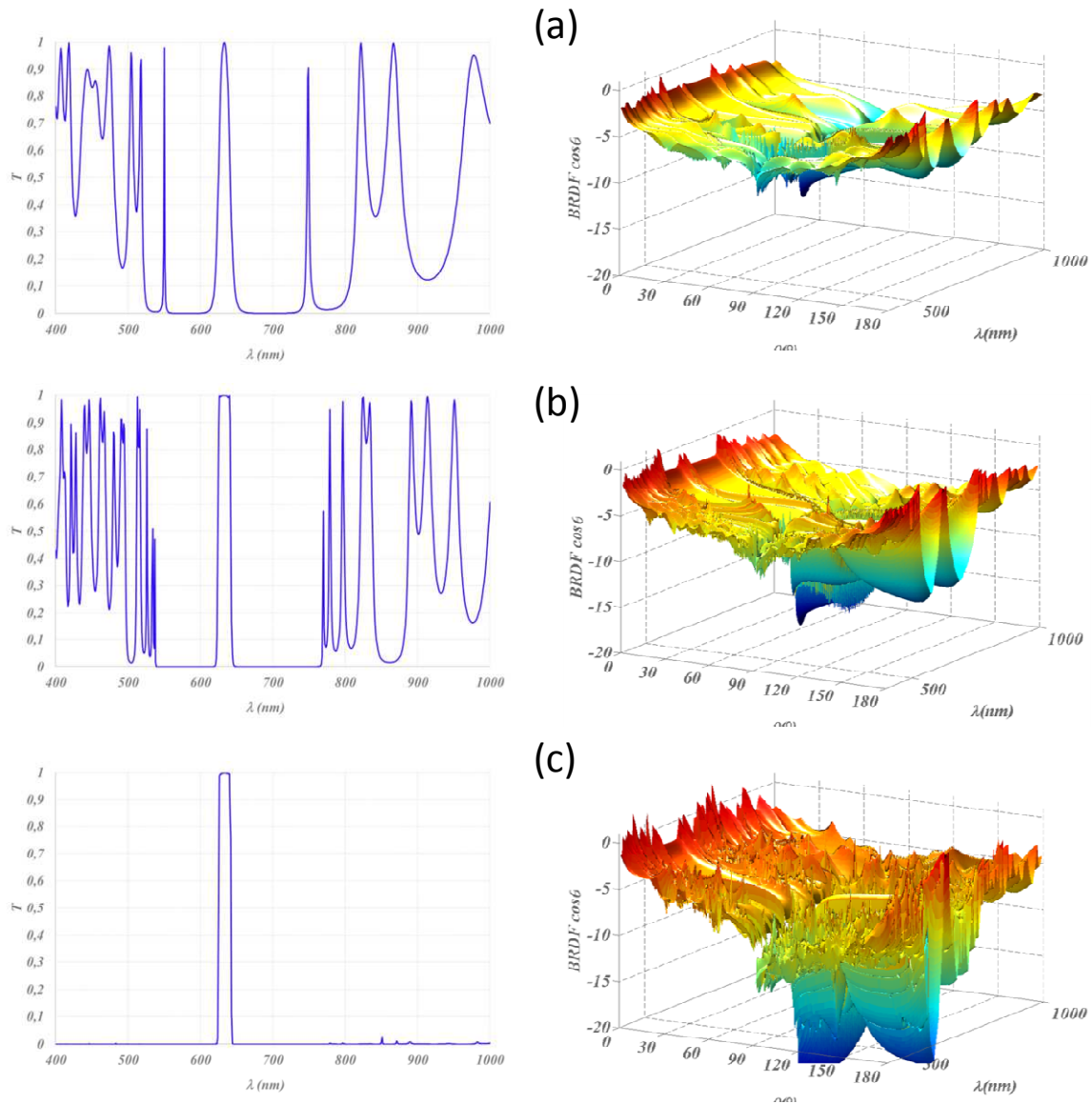


Figure 11: Spectral transmission (left) and spectral and angular of the intensity of light scattered (right) by three complex filters: (a) - a Fabry-Perot cavity, (b) - a multi-cavities Fabry-Perot filter and (c) - the same as (b) with self-blocking filters

We can see that, when the number of layers is increased, the scattering response is significantly complexified. More precisely, we can see on these graphs that scattering mappings (b) and (c) present a lot of scattering lobes whose location and amplitude cannot be predicted without an accurate numerical calculation. To be more quantitative, the angular scattering patterns in the incident plane are extracted for an illumination wavelength of respectively 570 nm and 633 nm. They are plotted Figure 12 and Figure 13.

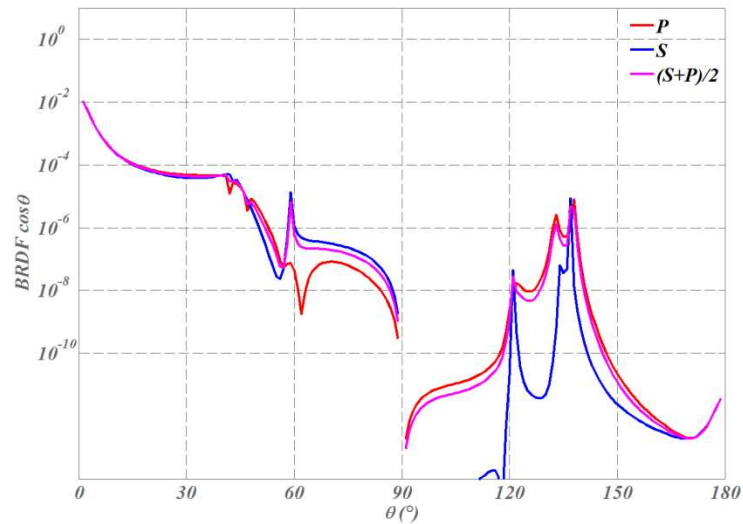


Figure 12 : Modelization of the angular pattern of the intensity of light scattered in the incident plane by a filter (b) presented in Figure 11 assumed to be deposited on the substrate measured Figure 2 under S and P polarization. Calculation is made for $\lambda=570$ nm

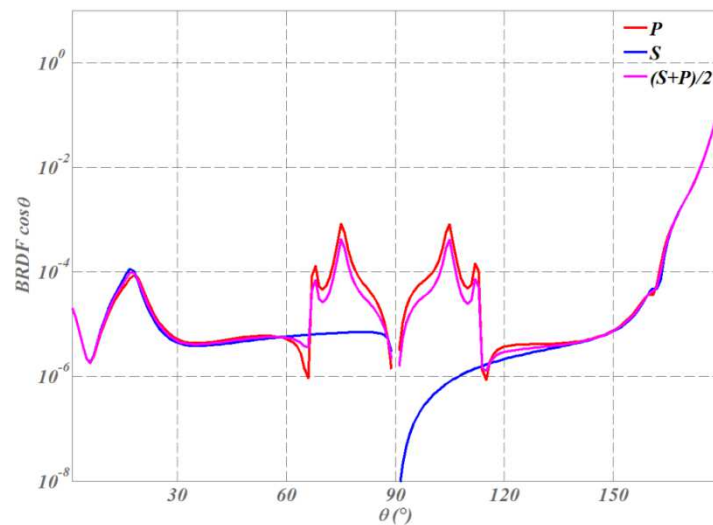


Figure 13 : Modelization of the angular pattern of the intensity of light scattered in the incident plane by a filter (b) presented in Figure 11 assumed to be deposited on the substrate measured Figure 2 under S and P polarization. Calculation is made for $\lambda=633$ nm

We can notice here that an enhancement- of scattering may occur at large angles. It can reach several decades and can be a source of cross-talk which cannot be neglected. This point is confirmed Figure 14 where we compared the spectral transmission of this filter (T in blue) to the total integrated scattering (TS in red). We can see on this graph that in the rejection band, the total scattered intensity is 3 decades higher than the transmission level. So, in this case, straylight becomes the main limitation to the performances of the filter.

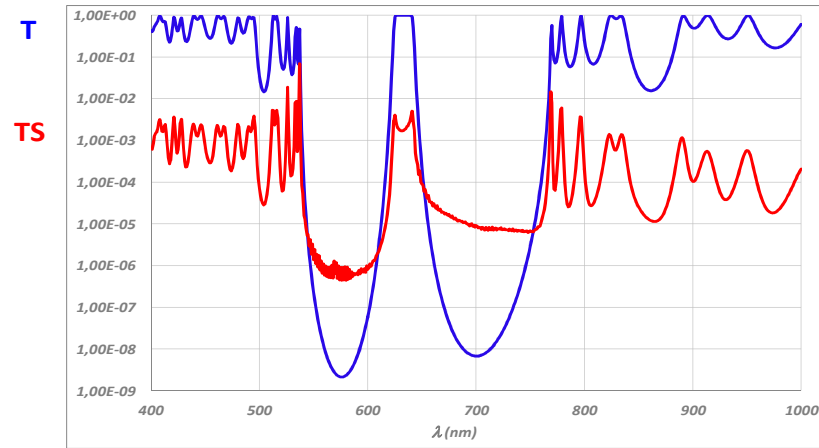


Figure 14: Spectral evolution of the transmission coefficient (T) and the Total integrated Scattering (TS) for filter (b) of Figure 7.

At last, to validate the accuracy of the model, the spectral and angular evolution of the scattered intensity of a complex multi-dielectric filter (> 100 layers) has been measured with SALSA instrument [1, 2, 13, 14, 20, 21]. The corresponding mapping is given Figure 15 (left) where it is compared to the modelization. Agreement between models and metrology is now excellent even in the localisation and estimation of the scattering lobes.

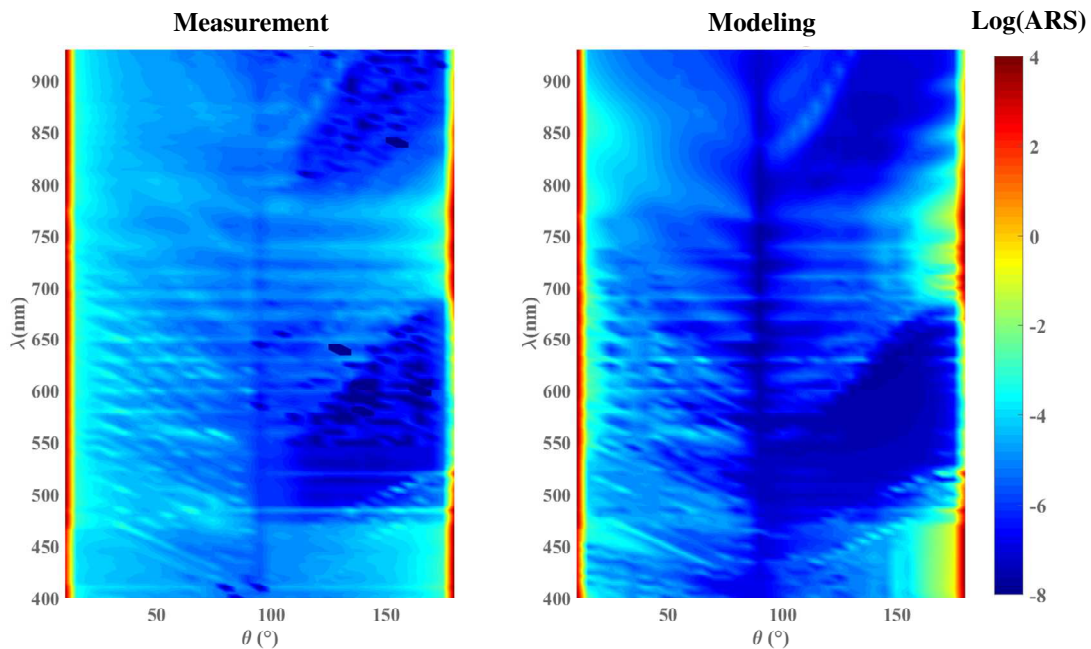


Figure 15: Modelization (right) and measurement (left) of the spectral and angular evolution of the intensity of the light scattered by a complex optical filter (> 100 layers)

6. CONCLUSION

Last developments performed at Institut Fresnel in terms of modelization of light scattered by optical coatings have been presented and compared to the metrology. Filters with high level of complexity can now be addressed and agreement between models and experiments is now highly successful, even for complex optical coatings (> 100 layers) and for

spectral and angular mappings. Now, these new facilities will be used by the scattering Group to work on a better management of light scattered by complex optical coatings.

Funding sources and acknowledgments. This work has been realized thanks to the support of the French National direction of armament (Direction Générale de l'Armement) and the French National Space Center (CNES). The authors also acknowledge the RCMO group of the Institut Fresnel for the realization of the complex filters.

7. REFERENCES

1. M. Lequime, S. Liukaityte, M. Zerrad, and C. Amra, "Ultra-wide-range measurements of thin-film filter optical density over the visible and near-infrared spectrum," *Optics Express* **23**, 26863-26878 (2015).
2. S. Liukaityte, M. Lequime, M. Zerrad, T. Begou, and C. Amra, "Broadband spectral transmittance measurements of complex thin-film filters with optical densities of up to 12," *Optics Letters* **40**, 3225-3228 (2015).
3. S. Liukaityte, M. Zerrad, M. Lequime, T. Bégou, and C. Amra, "Measurements of angular and spectral resolved scattering on complex optical coatings," (Proceedings of SPIE, 2015).
4. C. Amra, "First-order vector theory of bulk scattering in optical multilayers," *Journal of the Optical Society of America A* **10**, 365-374 (1993).
5. C. Amra, "From light scattering to the microstructure of thin-film multilayers," *Applied Optics* **32**, 5481-5491 (1993).
6. C. Amra, "Light scattering from multilayer optics. I. Tools of investigation," *Journal of the Optical Society of America A* **11**, 197-210 (1994).
7. C. Amra, "Light scattering from multilayer optics. II. Application to experiment," *Journal of the Optical Society of America A* **11**, 211-226 (1994).
8. J. M. Elson, and J. M. Bennett, "Relation between the angular dependence of scattering and the statistical properties of optical surfaces," *Journal of the Optical Society of America* **69**, 31-47 (1979).
9. J. M. Elson, J. P. Rahn, and J. M. Bennett, "LIGHT-SCATTERING FROM MULTILAYER OPTICS - COMPARISON OF THEORY AND EXPERIMENT," *Applied Optics* **19**, 669-679 (1980).
10. A. Duparre, and S. Kassam, "RELATION BETWEEN LIGHT-SCATTERING AND THE MICROSTRUCTURE OF OPTICAL THIN-FILMS," *Applied Optics* **32**, 5475-5480 (1993).
11. S. Schroder, T. Herffurth, A. Duparre, and J. E. Harvey, "Impact of surface roughness on scatter losses and the scattering distribution of surfaces and thin film coatings," in *Optical Fabrication, Testing, and Metrology Iv*, A. Duparre, and R. Geyl, eds. (2011).
12. S. Schroder, A. Duparre, L. Coriand, A. Tunnermann, D. H. Penalver, and J. E. Harvey, "Modeling of light scattering in different regimes of surface roughness," *Optics Express* **19**, 9820-9835 (2011).
13. M. Zerrad, S. Liukaityte, M. Lequime, and C. Amra, "Light scattered by optical coatings: numerical predictions and comparison to experiment for a global analysis," *Applied Optics* **55**, 9680-9687 (2016).
14. M. ZERRAD, M. LEQUIME, S. LIUKAITYTE, and C. AMRA, "Parasitic light scattered by complex optical coatings: modelization and metrology," *CEAS Space Journal* **9**, 473-484 (2017).
15. J. E. Harvey, S. Schroder, N. Choi, and A. Duparre, "Total integrated scatter from surfaces with arbitrary roughness, correlation widths, and incident angles," *Optical Engineering* **51** (2012).
16. C. Amra, and S. Maure, "Electromagnetic power provided by sources within multilayer optics: free-space and modal patterns," *Journal of the Optical Society of America A* **14**, 3102-3113 (1997).
17. C. Amra, and S. Maure, "Mutual coherence and conical pattern of sources optimally excited within multilayer optics," *Journal of the Optical Society of America A* **14**, 3114-3124 (1997).
18. C. Amra, C. Grèzes-Besset, and L. Bruel, "Comparison of surface and bulk scattering in optical multilayers," *Applied Optics* **32**, 5492-5503 (1993).
19. C. Deumié, R. Richier, P. Dumas, and C. Amra, "Multiscale roughness in optical multilayers: atomic force microscopy and light scattering," *Applied Optics* **35**, 5583-5594 (1996).
20. S. Liukaityte, M. Zerrad, M. Lequime, T. Begou, C. Amra, M. Lequime, H. Macleod, and D. Ristau, "Measurements of angular and spectral resolved scattering on complex optical coatings," in *Optical Systems Design 2015: Advances in Optical Thin Films V*(2015).
21. S. Liukaityte, M. Lequime, M. Zerrad, T. Begou, J. Lumeau, C. Amra, M. Lequime, H. Macleod, and D. Ristau, "Ultra-wide range system for the spectral transmission measurement of complex optical filters," in *Optical Systems Design 2015: Advances in Optical Thin Films V*(2015).